Dynamics of Fixed Bed Reactor with a Kinetically Controlled Complex Reaction*

by

Boris GOLMAN**, Shintaro FUJISAKI**, Tohru KANNO**
and Masayoshi KOBAYASHI**

(Received April 28, 1994)

(Abstract)

The dynamic behavior of a differential tubular flow reactor shows sometimes anomalous modes. One possible expramation for these complex modes has proposed by using a multi-path model reaction and superimposing the two response curves. The two most important factors to characterize the mode were found such as an initial condition of catalyst surface and the magnitude of the reactor stimulus.

Introduction

The classical kinetic analysis in heterogeneously catalyzed reaction was based on Langmuir-Hinshelwood-Hougen-Watson rate equations. This equations are useful in modeling of steady state single pathway catalytic reactions, but they cannot be used to describe the detailed kinetics of complex multiple-path reactions. The surface heterogeneity, lateral interaction and mobility of metal catalyst particle on real catalyst surface may reasonably induce multiple-path reaction.

Recently many works involving multiple-path reactions have been reported. An old example is the reaction between H_2 and O_2 on platinum to produce water as first studied by Faraday, and then by a very large number of investigators [1]. Tamaru et al. [2] demonstrated that CO oxidation on ZnO was consisted of two pathways. Fiolitakis and Hofmann [3] reported a three-path reaction kinetic model for the water-gas shift reaction on the oxidation state of a CuO/ZnO industrial catalyst. Kobayashi et al. [4-6] have demonstrated the two-path models for CO oxidation on various metal oxides and metals, MnO_2, Cr_2O_3, Pb_3O_4, ZnO and Ag, that are controlled by different active sites and adsorbed species.

It might be well to point out, that clarifying the detail of complex kinetics by using steady state rate data is difficult. The transient response method (TRM) [7, 8] has been recognized as a powerful tool for studying the mechanism of heterogeneously catalyzed

reaction.   The object of this investigation is to classify the complicated transient responses for model heterogeneously catalyzed multiple-path reactions by computer simulations.

Mathematical model and numerical techniques

In the present study, two-path reaction is considered as a simple example of complex multiple-path reactions.   There is only one overall reaction, but it may proceed by two different paths in parallel.

<div align="center">

path I

$X_1 + X_2$ ⟨ ⟩ Y

path II

</div>
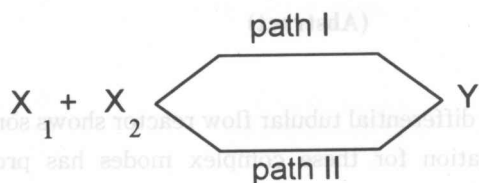
The reaction takes place in a tubular fixed-bed differential reactor.   The mathematical model employed here is a continuum, one-dimensional pseudo-homogeneous representation similar to the models of many earlier investigators [9].   The differential equations that describe isothermal plug flow reactor behavior can be derived from reaction mechanism assuming mass action kinetics, ideal plug-flow behavior and the absence of limiting transport effects:

$$-\frac{U}{p_cR_sT}\frac{\partial P_i}{\partial Z} - r_i = \frac{\varepsilon}{p_cR_sT}\left(\frac{\partial P_i}{\partial t}\right) \tag{1}$$

$$\frac{\partial c_w^*}{\partial t} = r_w \tag{2}$$

The balance equation for each type of active site

$$i^Tc_w^* = qm_w, \text{ where } i^T = [1, \cdots, 1] \tag{3}$$

can be used in obtaining the dimensionless quantity, the vector of fractional coverage:

$$\theta_w = c_w^*/qm_w \tag{4}$$

where qm_w is the surface adsorption capacity.   Equation (2) may be written as

$$\frac{\partial \theta_w}{\partial t} = \frac{1}{qm_w}r_w \tag{5}$$

Since the extent of reaction is small in the differential reactor, it may be assumed that the concentration of reactants and products is linearly distributed along the reactor length.   On the basis of this supposition, the distributed parameter system may be converted to a lumped parameter system.   Equations (1) and (5) may now be written as

$$\frac{d\bar{P}_i}{dt} = -\frac{2U}{\varepsilon L}\left(\bar{P}_i - P_i^0\right) - \frac{P_cR_sT}{\varepsilon}\bar{r}_i \tag{6}$$

$$\frac{d\bar{\theta}_w}{dt} = \frac{1}{qm_w}\bar{r}_w \tag{7}$$

where $\bar{r}_i$, $\bar{r}_w$ denote that the reaction rate has to be computed with mean concentration in the reactor. The outlet concentration, P_i, can be expressed by the arithmetic mean concentration $\bar{P}_i$:

$$P_i = 2\bar{P}_i - P_i^0 \tag{8}$$

The initial conditions for Equations (6) and (7) are

$$P_i^0 = f(0) \quad at \ t = 0 \tag{9}$$

$$P_i = P_i^{st} \quad at \ t = 0 \tag{10}$$

$$\theta_w = g(0) \quad at \ t = 0 \tag{11}$$

Equation (9) gives the initial conditions at the inlet of the reactor and Equation (10) gives those at the outlet of the reactor. Conditions (11) are for the fractional surface coverage of adsorbed species at the initial steady state. The function $g(0)$ can be determined from the steady state solution of Equations (7).

In the following, let us designate X-Y response as the response of product Y in the effluent stream to the stepwise change of reactant X in the feed. When X is increased from P_X^A to P_X^B, the response is marked as X(inc., P_X^A, P_X^B)-Y, and when X decreased from P_X^B to P_X^A, as X(dec., P_X^B, P_X^A)-Y.

The coupled system of ordinary differential equations (ODEs) (6) and (7) with initial conditions (9)–(11) was solved numerically using a computer simulation package. This software package contains the library of reliable algorithms for solving ODEs [10]. For our simulation we have chosen a method based on the set of stiffly-stable backward differentiation formulas developed by Gear for stiff problems. In non-stiff cases an explicit multi-value Adams-Moulton and Runge-Kutta methods were used. All of the methods can dynamically change the order of the formula of integration and a step size for efficiency and accuracy. The library also consists of the algorithm for automatically switches between Adams-Moulton and Gear methods, depending on the stiffness of the system ODEs [11].

Simulations are carried out with an interactive program package which has been written in MS Fortran 77 for the computer DECpc 433dxLP. The reactor parameters used in the computer simulation are presented in Table 1.

Table 1. Parameter values for computer simulations

Reaction temperature (T)	423°K
Superficial gas velocity (U)	200 cm/min
Reactor length (L)	50 cm
Catalyst bed density (P_c)	1.0 g/cm³
Void fraction of packed bed reactor (ε)	0.5
Saturated amount of adsorbed species on the catalyst surface (qm_i)	1.0×10^{-6} mol/g

Simulation of transient responses for model multiple-path reactions

Model reaction 1.

The first example includes a dual route reaction system with different paths causes to the same overall reaction. We assume that reaction simultaneously proceeds on two different active sites S_1 and S_2 and the adsorbed species on S_1 and S_2 are independent of each other. Along both reaction pathways a reactant X_2 is adsorbed on the surface ($X_2 \cdot S_1$ and $X_2 \cdot S_2$) and reacts with adsorbed $X_1 \cdot S_1$ (Langmuir-Hinshelwood path I) or with gaseous X_1 (Eley-Rideal path II). We now assume that both reaction paths are controlled by the surface reaction and that adsorbed Y is liberated very fast from the surface. The dual path mechanism may be written:
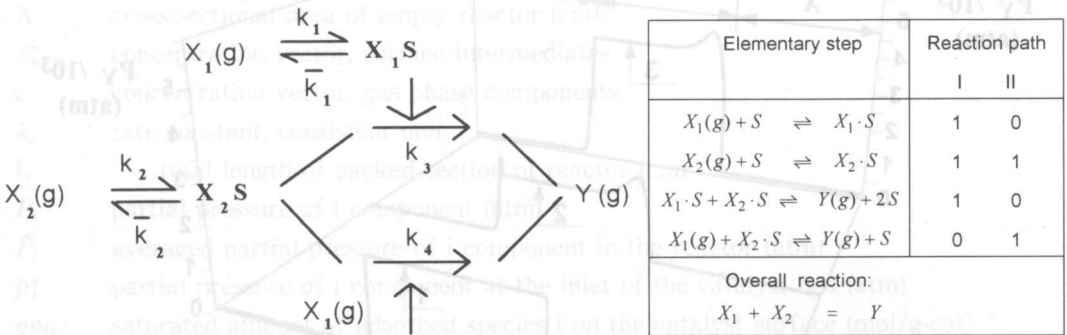
$$X_1(g) \underset{k_{-1}}{\overset{k_1}{\rightleftharpoons}} X_1 S_1$$

$$X_2(g) \underset{k_{-2}}{\overset{k_2}{\rightleftharpoons}} X_2 S_1 \xrightarrow{k_3}$$

$$X_2(g) \underset{k_{-4}}{\overset{k_4}{\rightleftharpoons}} X_2 S_2 \xrightarrow{k_5}$$

$$\longrightarrow Y(g)$$

$$X_1(g)$$

Elementary step	Reaction path	
	I	II
$X_1(g) + S_1 \rightleftharpoons X_1 \cdot S_1$	1	0
$X_2(g) + S_1 \rightleftharpoons X_2 \cdot S_1$	1	0
$X_2(g) + S_2 \rightleftharpoons X_2 \cdot S_2$	0	1
$X_1 \cdot S_1 + X_2 \cdot S_1 \rightleftharpoons Y(g) + 2 S_1$	1	0
$X_1(g) + X_2 \cdot S_2 \rightleftharpoons Y(g) + S_2$	0	1
Overall reaction:		
$X_1 + X_2 = Y$		
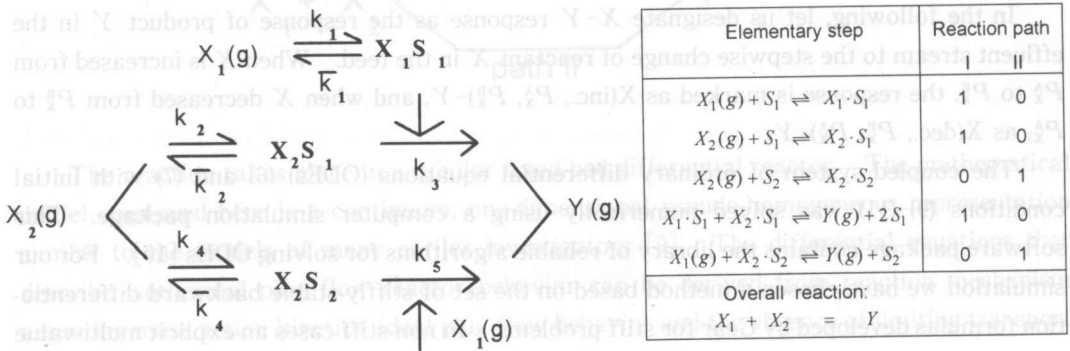
The X_1(inc., 0.01)-Y and X_1(dec., 0.01)-Y responses were simulated by changing the values of rate constants k_3 and k_5. The step responses of Y in different cases are shown in figure 1. It should be emphasized the difference between step responses for cases 1 and 2, which corresponds to a slow Langmuir-Hinshelwood and Eley-Rideal step, respectively. Curve I in Figure 1 shows an instantaneous mode. This may be attributed to the slow surface reaction and rapid adsorption of X_1. In case 2 the Eley-Rideal mechanism dominates and the slight overshoot is evident. Curve 3 indicates an overshoot mode. In this case the Eley-Rideal mechanism dominates at the initial stage because the component X_1 must first be adsorbed on the catalyst surface for Langmuir-Hinshelwood step.

Model reaction 2.

This model reaction system also includes a dual route reaction with different paths leading to the same overall reaction. Path I goes through Langmuir-Hinshelwood elementary steps where two adsorbed species ($X_1 \cdot S$ and $X_2 \cdot S$) react together. Path II involves an Eley-Rideal step, i. e., a reaction between a surface species ($X_2 \cdot S$) and a gaseous species (X_1 (g)). By contrast with previous example, the same type of active sites is involved for both routes in which X_1 and X_2 are competitively adsorbed on S. Reactant X_2 is assumed to be preadsorbed on the surface causing $X_2 \cdot S$ to occupy totally the sites on the catalyst surface.

The following dual path mechanism is considered:

$$X_1(g) \underset{\overline{k_1}}{\overset{k_1}{\rightleftharpoons}} X_1 S$$

$$X_2(g) \underset{\overline{k_2}}{\overset{k_2}{\rightleftharpoons}} X_2 S$$

$$X_1(g)$$

Elementary step	Reaction path	
	I	II
$X_1(g) + S \; \rightleftharpoons \; X_1 \cdot S$	1	0
$X_2(g) + S \; \rightleftharpoons \; X_2 \cdot S$	1	1
$X_1 \cdot S + X_2 \cdot S \rightleftharpoons Y(g) + 2S$	1	0
$X_1(g) + X_2 \cdot S \rightleftharpoons Y(g) + S$	0	1
Overall reaction:		
$X_1 + X_2 \;\; = \;\; Y$		

The X_1-Y responses were simulated for different values of rate constants k_3 and k_4. The results obtained are displayed in Figure 2. Curve 1 in Figure 2 shows a monotonic increase mode, which corespondents to a slow Langmuir-Hinshelwood step. In the case 2 the overshoot is observed. The overshoot mode are ascribed to the slow Eley-Rideal mechanism. The curve 3 visualize the complex mode. The complex mode arises from the superposition of two parts complying with different reaction paths with competitive adsorption of reaction components. One is an instantaneous increase at the initial stage of the response and the other is a successive overshoot with a gradual maximum. The instantaneous response at the initial stage are conformed to the prevalence of Eley-Rideal step because adsorbed X_1 is not available for the Langmuir-Hinshelwood step. The influence of the Langmuir-Hinshelwood step is increased because X_1 is accumulated on the catalyst surface and overshoot mode is observed.

By this means it is possible to distinguish between the dominance of either Eley-Rideal or Langmuir-Hinshelwood reaction step for multiple-path reaction by analysis of the shape of the product response.

Conclusions

The analysis of the complicated transient responses for model heterogeneously catalyzed multiple-path reactions has been accomplished. The mode of the transient responses of products caused by the concentration step-change of reactants has been classified depending on the combination of the kinetic parameters.

No.	k_1	$\overline{k_1}$	k_2	$\overline{k_2}$	k_3	k_4	$\overline{k_4}$	k_5
1	1.0×10^{-4}	1.0×10^{-7}	1.0×10^{-4}	1.0×10^{-7}	1.0×10^{-8}	1.0×10^{-4}	1.0×10^{-7}	1.0×10^{-6}
2	_″_	_″_	_″_	_″_	1.0×10^{-6}	_″_	_″_	1.0×10^{-8}
3	_″_	_″_	_″_	_″_	1.0×10^{-6}	_″_	_″_	1.0×10^{-6}

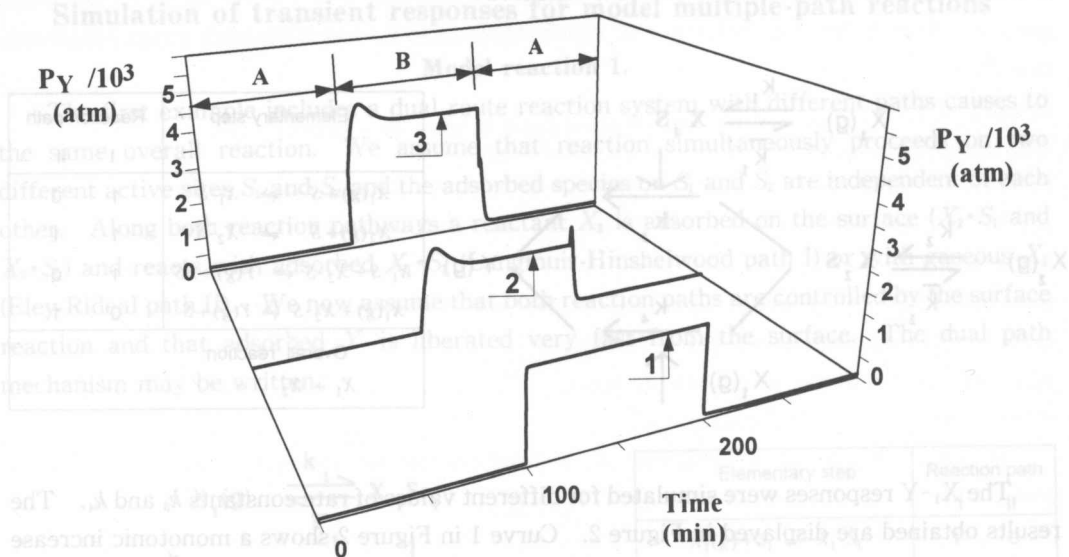**Figure 1.** X_1-Y response for model reaction 1. Conditions:
P_{X_2} = 0.2 atm, A, $P_{X_1}^A$ = 0.01 atm, B, $P_{X_1}^B$ = 0.25 atm.

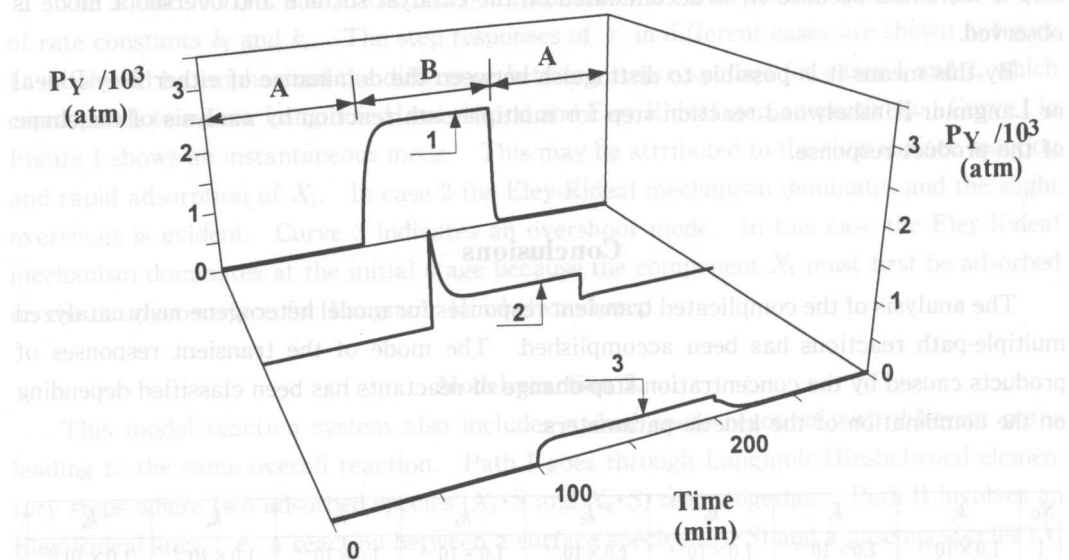| No.	k_1	$\bar{k}_1$	k_2	$\bar{k}_2$	k_3	k_4
1	1.0×10^{-4}	1.0×10^{-7}	1.0×10^{-4}	1.0×10^{-7}	1.0×10^{-8}	1.0×10^{-6}
2	_ $''$ _	_ $''$ _	_ $''$ _	_ $''$ _	1.0×10^{-6}	1.0×10^{-8}
3	_ $''$ _	_ $''$ _	_ $''$ _	_ $''$ _	1.0×10^{-7}	1.0×10^{-7}

Figure 2. X_1-Y response for model reaction 2. Conditions: P_{X_2} = 0.2 atm,
A, $P_{X_1}^A$ = 0.01 atm, B, $P_{X_1}^B$ = 0.2 atm.

Notation

A   cross-sectional area of empty reactor (cm²)

c_w^* concentration vector, surface intermediates

c   concentration vector, gas phase components

k_s rate constant, consistent unit

L   total length of packed section of reactor (cm)

P_i partial pressure of i component (atm)

$\bar{P}_i$ averaged partial pressure of i component in the reactor (atm)

p_i^0 partial pressure of i component at the inlet of the catalyst bed (atm)

qm_w saturated amount of adsorbed species i on the catalyst surface (mol/g-cat)

r   component production rate vector

Rs   gas constant, consistent unit

T   temperature, K

t   time (min)

U   superficial gas velocity (cm/min)

Z   distance along reactor length (cm)

$f(0)$ initial partial pressure distribution of component i as a function of reactor length

$g(0)$ initial fraction of catalyst monolayer distribution of component w as a function of reactor length

Greek symbols

p_c bulk catalyst density (g-cat/cm³-reactor)

ε void fraction of packed section of the reactor, dimensionless

θ_w fraction of catalyst monolayer covered with w component (dimensionless)

$\bar{\theta}_w$ averaged surface coverage of w component (dimensionless)

References

1.   Hanson, F. V. and Boudart, M. 1978. J. Catalysis 53, 56.
2.   Ohtsuka, K., Tanaka, K., and Tamaru, K. 1967. Nippon Kagaku Zasshi 88, 830.
3.   Fiolitakis, E. and Hofmann, H. 1983. J. Catalysis 80, 328.
4.   Kobayashi, M. and Kobayashi, H. 1972. J. Catalysis. 27, 100, 108, 114.
5.   Kobayashi, M. and Kobayashi, H. 1976. Bull. Chem. Soc. J. 49, 3009, 3014, 3018.
6.   Golman, B., Kasai, A., Kanno, T. and Kobayashi, M., 1993. Memoirs of KIT. 25, 49.
7.   Kobayashi, H. and Kobayashi, M. 1974. Catal. Rev. Science and Eng. 10, 139.
8.   Kobayashi M , 1982. Chemical Engineering Science. 37, 393.
9.   Lehr, C. G., Yurchak, S. and Kabel, R. L. 1968. AICHE journal. 14, 627.
10.   Tanaka, H., Hakozaki, M., Kanno, T., Golman B. and Kobayashi, M.. Personal computer simulation package for the analysis of multi-reaction pathways in heterogeneous catalysis. Proc. Computer aided Innovation of New Materials II, Yokohama, Sep. 22-25, 1992. Eds. M. Doyama, J. Kihara, M. Tanaka and R. Yamamoto. 1993. North-Holland, Elsevier. Part 2. p. 1065-1068.
11.   Kahaner, D., Moler, C. and Nash, S. 1988, Numerical methods and software, Prentice Hall, New Jersey.